Annales Geophysicae (2003) 21: 719–728

Annales Geophysicae

Rocket-borne investigation of auroral patches in the evening sector during substorm recovery

M. A. Danielides[1] **and A. Kozlovsky**[1, 2]

[1]Department of Physical Sciences, P.O. Box 3000, FIN-90014 University of Oulu, Finland
[2]Sodankylä Geophysical Observatory, FIN-99600 Sodankylä, Finland

Received: 13 May 2002 – Revised: 6 August 2002 – Accepted: 11 September 2002

Abstract. On 11 February 1997 at 08:36 UT after a substorm onset the Auroral Turbulence 2 sounding rocket was launched from Poker Flat Research Range, Alaska into a moderately active auroral region. This experiment has allowed us to investigate evening (21:00 MLT) auroral forms at the substorm recovery, which were discrete multiple auroral arcs stretched to, the east and southeast from the breakup region, and bright auroral patches propagating westward along the arcs like a luminosity wave, which is a typical feature of the disturbed arc. The rocket crossed an auroral arc of about 40 km width, stretched along southeast direction. Auroral patches and associated electric fields formed a 200 km long periodical structure, which propagated along the arc westward at a velocity of 3 km/s, whereas the ionospheric plasma velocity inside the arc was 300 m/s westward. The spatial periodicity in the rocket data was found from optical ground-based observations, from electric field in situ measurements, as well as from ground-based magnetic observations. The bright patches were co-located with equatorward plasma flow across the arc of the order of 200 m/s in magnitude, whereas the plasma flow tended to be poleward at the intervals between the patches, where the electric field reached the magnitude of up to 20 mV/m, and these maxima were co-located with the peaks in electron precipitations indicated by the electron counter on board the rocket. Pulsations of a 70-s period were observed on the ground in the eastern component of the magnetic field and this is consistent with the moving auroral patches and the north-south plasma flows associated with them. The enhanced patch-associated electric field and fast westward propagation suggest essential differences between evening auroral patches and those occurring in the morning ionosphere. We propose the wave that propagates along the plasma sheet boundary to be a promising mechanism for the evening auroral patches.

Key words. Ionosphere (auroral ionosphere; electric fields and currents)

Correspondence to: M. A. Danielides
(michael.danielides@oulu.fi)

1 Introduction

Magnetospheric substorm onset (e.g. Akasofu, 1964; Rostoker et al., 1980) is accompanied by a fast change in the magnetospheric configuration, after which a recovery occurs toward a new steady state. The onset is manifested by a brightening and expansion of the auroral oval, which is associated with discrete auroral structures developing toward the west and the east, and also equatorward from the breakup region (Nakamura et al., 1993). Later, during the recovery, the discrete auroral structures develop into diffuse and pulsating auroras.

At the substorm recovery, typical auroral forms are the discrete auroral structures (Nakamura et al., 1993) and pulsating auroras (e.g. Davis, 1978; Johnstone, 1983). The pulsating auroras are more prevalent in the midnight and morning sectors, but at the recovery of the substorm they are observed in the evening sector as well, occurring as patches and arc segments (Royrvik and Davis, 1977). The pulsating patches have a size from about 10 to 200 km in diameter. Usually they are found in irregular shapes. Royrvik and Davis (1977) reported auroral patches from simple to more complex structures of any orientation. Their periods of pulsations are in the period range from several to tens of seconds. The auroral patches drift eastwards in the morning sector and westwards in the evening sector. Arc segments usually show no internal structure and can be considered as uniform, sharply bounded and spatially stable. The size varies from 1 to 10 km wide and of the order of 100 km long in any orientation (Royrvik and Davis, 1977). The arc segments may develop from the arc-like discrete auroral structures described by Nakamura et al. (1993).

There were many efforts made to understand the mechanisms of the substorm onset (see, e.g. reviews by Elphinstone et al., 1996; Rostoker, 1999; Lui, 2001). However, less attention was paid to the auroral structures arising at the substorm recovery, due to turbulence in the magnetosphere-ionosphere

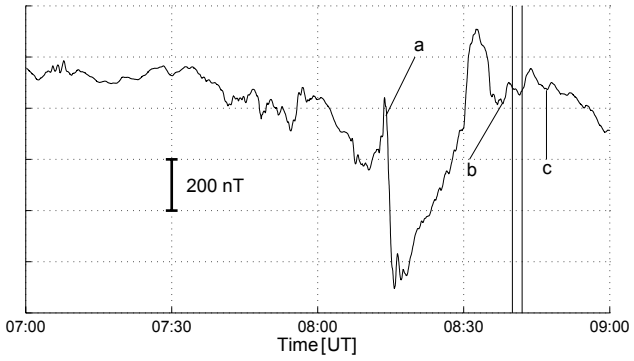

Fig. 1. Magnetic X-component for Poker Flat, Alaska on 11 February 1997 from 07:00 to 09:00 UT. The times a, b, c are indicating the times of POLAR satellite coverage (Fig. 2). The time interval 08:40 to 08:42 UT discussed within this study is marked at the substorm recovery.

system. These complex and highly variable auroras can be well observed by optical instruments, but one has seldom the possibility to measure the electric fields (or the F-region ionospheric plasma flows) associated with them. Incoherent scatter radar provides good data on the plasma flows associated with stable auroral forms (Aikio et al., 1993), but in the disturbed background the radar measurements are hardly running at a proper temporal resolution. Sometimes outside the discrete auroral structures one finds large electric fields, such as described in Lanchester et al. (1996). These higher electric fields are found in regions of low electron density and, therefore, with a low signal-to-noise ratio leads to still one difficulty with radar measurements. Thus, low-altitude satellite and rocket-born experiments would be the best tools for the investigation of the auroral activity during the substorm recovery phase, but such measurements are rather seldom. Mainly in situ electric fields related to auroral arcs have been studied in the past (Marklund, 1984). In this paper we report on the unique observations made in the course of the Auroral Turbulence 2 (AT2) rocket experiment, which allow us to study the electrodynamics of the auroral structures at the substorm recovery.

2 Instruments and data

On 11 February 1997 at 08:36 UT after a substorm onset the Auroral Turbulence 2 (AT2) sounding rocket was launched from Poker Flat Research Range, Alaska (64.9° N, 212.2° E, 21:00 MLT) into a moderate actively nightside auroral region and into the wake of the westward travelling surge (WTS). It was the first successful launch of a set of three slowly separating completely instrumented payloads (referred to as Main (central), North, and East) from a single launch vehicle (Black Brant XII), which flew in a triangle formation of observation points and crossed several distinct auroral forms during its 800 km flight. The payload cluster was remaining above the 150 km altitude for at least 600 s. The apogee was at around 500 km altitude. A detailed description of the experiment can be found in Pietrowski et al. (1999); Lynch et al. (1999); Danielides et al. (1999). In this study we use data from electric field and particle measurements on board this payload cluster.

For the electric field measurements, on board each payload four electric potential spheres were deployed on the ends of 1.5 m booms in the spin plane (Pietrowski et al., 1999). Here we leave the main payload out of consideration, due to contamination from the attitude control system (ACS) firings during the period of interest. The shadow effect in the raw electric field data for the sub-payloads has been equally treated as in Pietrowski et al. (1999). Since the North payload observes a greater shadow effect here, primarily the data from the East payload are considered. The raw electric field data is despun, using a rigid body motion model derived from the onboard magnetometer data (Ivchenko et al., 1999). The electric field data have been filtered by averaging over a 2-s window, in order to reduce the spiky signal structure caused by the shadow effect. In addition to the electric field data, the particle data (electron counts) are used in this study. The particle detectors measured 5 eV – 15 keV electrons, at all pitch angles (for more details, see Lynch et al., 1999).

Auroral observations were made by the all-sky TV cameras situated at Poker Flat rocket range (64.9° N, 212.2° E) and Fort Yukon (66.6° N, 214.8° E). The field of view (180°) of the camera is of the order of 500 km at 100 km altitude, overlapping and covering the region along the rocket trajectory without any gap. For our study, we used the time resolution of one frame every 5 s.

The altitude of the auroral luminosity was determined by triangulation from TV cameras (at Poker Flat and Fort Yukon) at about 105 km, whereas the rocket experiment was at the altitude of 360 km to 480 km. To determine the position of the payload with respect to the auroral structures, we mapped the payload position down to 105 km (auroral altitude) along the magnetic field lines. The National Space Science Data Center (NSSDC) transformation from Corrected GeoMagnetic (CGM) to GEOcentric spherical (geographic) coordinates has been used for this purpose.

The ultraviolet imager (UVI) on board the POLAR satellite was used for a global view of the auroral oval. Geomagnetic background and ionospheric electrodynamics were monitored by the ground-based magnetometer measurements. The magnetometers were located in Poker Flat and Fort Yukon, together with the all-sky TV cameras mentioned above.

3 Observations

The observations occurred in disturbed geomagnetic conditions (daily $A_p = 211.15$). Geophysical background of the investigated substorm was described in detail by Danielides et al. (1999). At about 08:13 UT a sharp decrease of about 700 nT occurred at Poker Flat in the magnetic H-component indicating a substorm onset (Fig. 1). The auroral breakup oc-

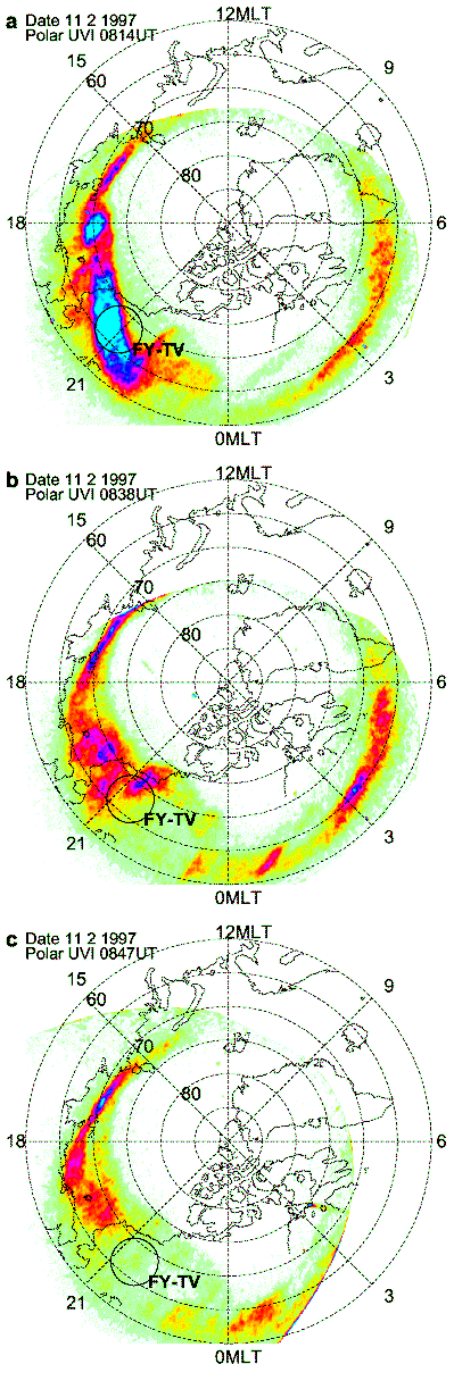

Fig. 2. Rendered projection of the POLAR satellite ultraviolet imager for **(a)** 08:14 UT, **(b)** 08:38 UT, as well as **(c)** 08:47 UT on 11 February 1997 on the northern polar cap. The coastline of Alaska is shown in the lower left quadrant. A westward travelling surge wake is found close to the northern coast of Alaska. The AT2 rocket experiment was launched into this region towards North. The field of view for the Fort Yukon TV all-sky camera (FY-TV) in Alaska is marked. Generally, the location of the auroral oval can be seen.

curred in the vicinity of the launch region. It was seen in a sequence of ultraviolet images obtained from the Polar satellite (three frames are presented in Figs. 2a–c).

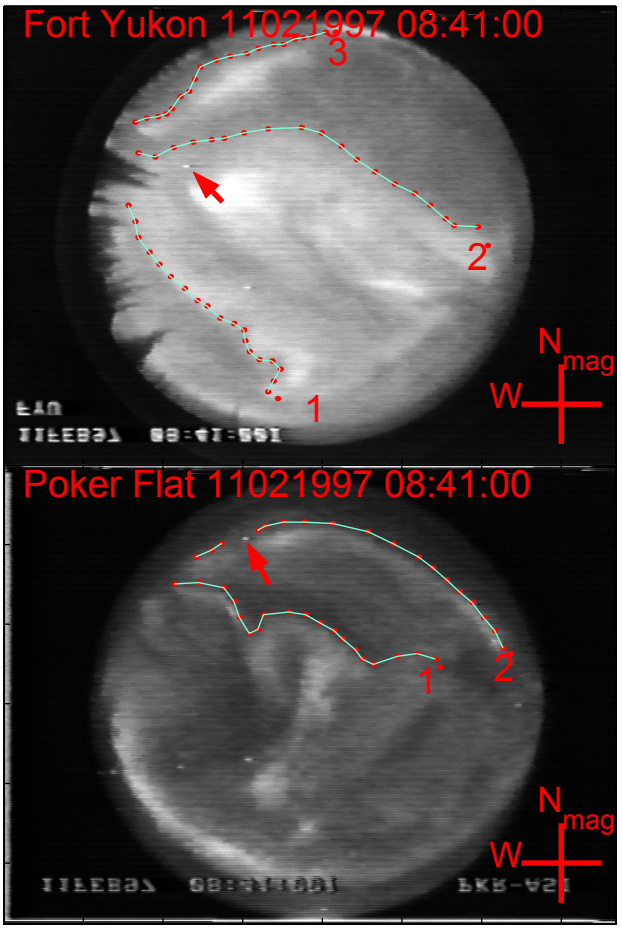

Fig. 3. The auroral display seen on a ASC frame at 08:40:00 UT on 11 February 1997 from Fort Yukon (upper frame) as well as from Poker Flat (lower frame), stations in Alsaka/US. North is up and East is right on the ASC frames. For the selected auroral structures 20 points connected by a line are covering the lower edge for the auroral arcs 1 to 3 in Fort Yukon, as well as 1 and 2 for Poker Flat.

At 08:36 UT, 23 min later after the substorm onset, the AT2 sounding rocket was launched into the WTS wake environment. Two global UV images taken at 08:38 and 08:47 UT (Figs. 2b and c) demonstrate the auroral background during the experiment, which was characterised by a gradual decreasing of the auroral activity. The circle near 21:00 MLT indicates the field of view of the all-sky camera in FY, which corresponds to the region of the observations reported here. Two ASC frames from FY and PF taken at 08:41 UT (Fig. 3) show more detailed auroral background along the rocket trajectory (arrows indicate the rocket position mapped along the magnetic field line to 105 km altitude). Three distinct arc-like auroral structures are indicated in Fig. 3 (arcs 1 and 2 are seen in both PF and FY).

Assuming the lower edge of the auroral luminosity at 105 km, we have mapped the selected three arcs onto a geographic map in Fig. 4, where the rocket trajectory crossing the auroral arcs 1, 2, and 3 is indicated by the line pointing northward from Poker Flat. The AT2 payload cluster deliv-

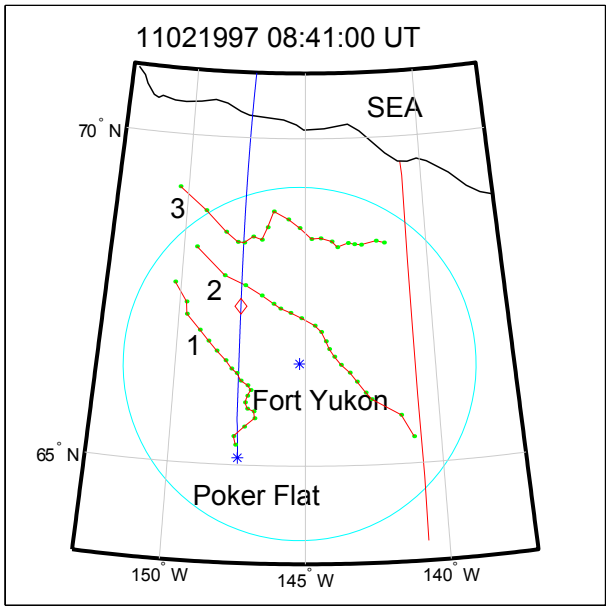

Fig. 4. Geog. map of Alaska, showing stations Poker Flat and Fort Yukon. The AT2 rocket trajectory, as well as the field of view for the Fort Yukon ASC station is shown. The position of the AT2 payloads is marked (diamond) for 11 February 1997 at 08:41:00 UT, as well as the auroral structures under investigation, sketched as a geographic projection. There are arcs numbered from 1 to 3 as discussed in the text.

ered useful in situ data, starting from about 08:40 UT when it was in a vicinity of arc 2. The entire set of AT2 measurement data has been studied earlier for a later period of the rocket flight (Danielides et al., 1999; Lynch et al., 1999; Ivchenko et al., 1999; Pietrowski et al., 1999). However, so far only the most intense large-scale auroral signatures have been studied, which were crossed by the payloads after 08:42 UT and are related to the most poleward arc 3. In the present study our main focus is on arc 2 and the associated fine auroral structures, which were crossed at around 08:40 to 08:42 UT.

The observed auroral arcs are typical discrete auroral structures developing within the bulge expanding poleward during a substorm, as was described by Nakamura et al. (1993) (p. 5743): "At the eastern part of the bulge, thin auroral features propagate eastward from the breakup region. Around the central meridian of the bulge, auroral features expand equatorward and become north-south aligned (the N–S aurora). The N–S aurora and the eastward propagating aurora develop into diffuse and pulsating aurora after the expansion." In Figs. 3 and 4, the most poleward intensive arc 3 corresponds to the aurora propagating eastward. This arc studied in earlier papers was quite stable, whereas arc 1 can be identified as "N–S" auroras decayed at the substorm recovery by developing into diffuse and pulsating aurora (Nakamura et al., 1993). Arc 2 is orientated in the NW–SE direction.

In the following sections we present a detailed investigation of the electric field and fine auroral structures associated with arc 2, which was crossed by the payload at around 08:40 to 08:42 UT, during the substorm recovery.

4 Data analysis and experimental results

Nine all-sky video frames from Fort Yukon in Fig. 5 show the auroral situation along the rocket trajectory at 08:40 to 08:42 UT. In the west part of the frames, the rocket position (mapped along the magnetic field line to 105 km altitude) is shown, together with its local geographical coordinate system, and vectors in the rocket location represent the in situ measured electric field. Thus, Fig. 5 shows the rocket when crossing arc 2. The arc was not homogeneous along its stretching: bright patches (indicated by letters a, b, and c) were propagating westward along the arc, so that patches (a) and (b) where passing close to the payload position at about 08:40:35 UT and 08:41:10 UT, respectively. The spatial size of the patches was of the order of 100 km. Arc 1 observed in the southwest was associated with patch-like bright structures, too. In the course of the observations, arcs 1 and 2 decayed by developing into the auroral patches and arc segments in a diffuse background.

For a more detailed consideration, we have mapped onto the Earth's surface the auroral structures associated with arc 2. Sketches in Fig. 6 show a sequence of the aurora positions in the rectangular framework having its origin in Fort Yukon and vertical axis pointed to the geomagnetic pole. The main interest is focused on the locations of arc 2 and the bright spots (patches a, b, and c) moving along this arc. The location of the auroras is represented by the position of its lower edge (assumed at the 105 km height), which is the sharp edge most distant from zenith at TV frames. The locations of the lower edge were determined several times manually for each frame; this has allowed us to find the average values and to estimate the error values, which were of the order of 20 km. The error bars create the strip-like sketch of the auroral arc in Fig. 6. The arc was oriented from northwest to southeast at an angle of about 20 degrees from geomagnetic latitude. Most intense luminosity regions of patches a and b are marked by asterisks with corresponding letters. The patches propagated to the west at a velocity of about 3 km/s, following each other at a distance of the order of 200 km along the arc. At the interval between patches (b) and (c), the auroral arc forms a fold-like structure bowed northward.

The location of the rocket is marked on the grid in Fig. 6 as a dot with a vector, where the vector represents the plasma drift velocity, $V = \boldsymbol{E} \times \boldsymbol{B}/B^2$, calculated from the in situ electric field measurement. The plasma drift velocity vectors from Fig. 6 are presented in an arc-associated coordinate system in Fig. 7a. The plasma drift velocity vectors form a vortex structure with its focus westward of the auroral patch, indicated as (b). This vortex structure is caused due to both the occurrence of an auroral arc associated electric field and an auroral patch associated electric field. One can separate the plasma velocity vectors into 2 components corresponding to the plasma flows along the arc (Vy) and across the arc (Vx) in the arc-associated coordinate system. The auroral patch,

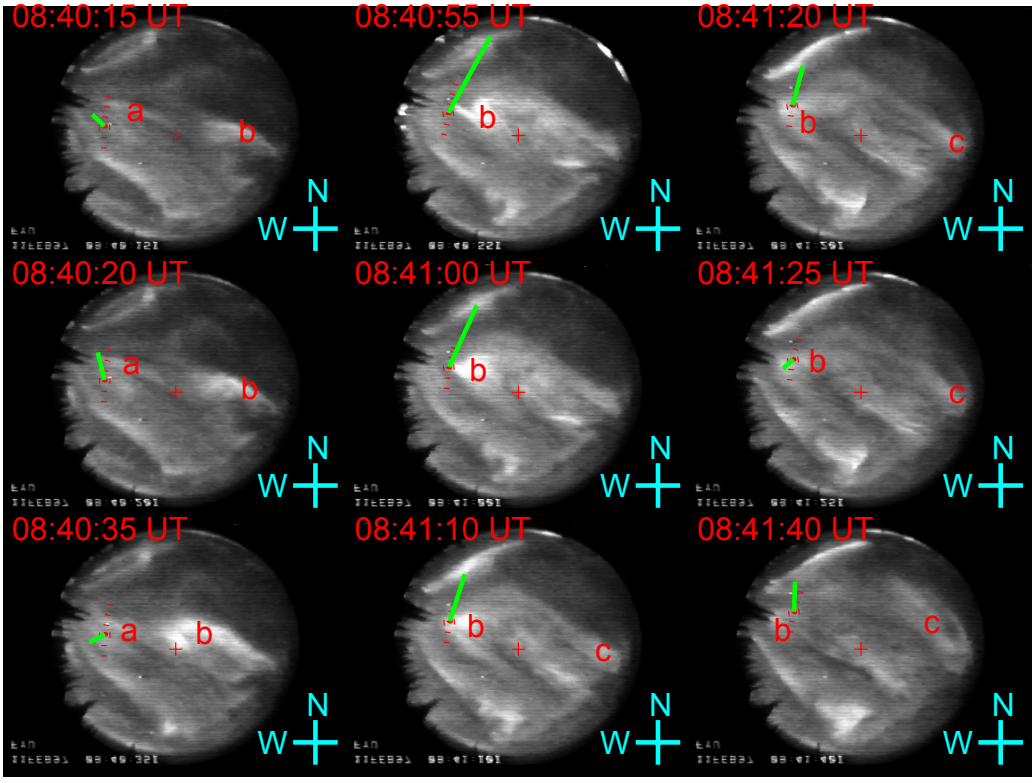

Fig. 5. The nine all-sky video frames are showing the auroral situation from 08:40:15 to 08:41:40 UT on 11 February 1997 at Fort Yukon station. Geomagnetic north is up, geomagnetic east on the right and the centre of each frame is marked with a little cross. In the northwest the rocket position is shown, together with its local geographical coordinate system. The in situ electric field is added to each frame. The auroral situation is active and several different luminosity auroral structures a to c are marked.

indicated as (b), is taken as a local reference point within the auroral arc structure. Then the auroral patches, indicated as (a) and (c), are shown in their mean distance to (b). Spatial variations in the cross-arc plasma flow (Vx) should be attributed to the inhomogeneous structures distributed along the arc.

Also, we have presented Vx in the framework of moving patches (Fig. 7b). This plot demonstrates that the auroral patches were associated with equatorward plasma flow (across the arc) of the order of 200 m/s in magnitude, whereas at the intervals between the patches the cross-arc plasma flow comes down to zero and tends to be poleward.

Figure 7c shows the plasma velocity component along the arc (Vy) versus a distance from the northern edge of the arc. This plot demonstrates that the arc was associated with a westward ionospheric plasma flow of the order of 300 m/s in magnitude, and convection reversal occurred at the northern edge of the arc. So, just poleward of the arc the plasma flow was eastward at about 200 m/s in magnitude. Thus, the arc corresponds to a Birkeland current type arc, after the classification of Marklund (1984).

Figure 8 summarises the measurements made during the rocket flight at 08:40–08:42 UT. In the considered initial stage of the flight, the separation between the payloads was small, so data of the North payload, showing only minor differences from East payload, are not presented here. A relative auroral intensity at the payload position, from 08:40:00 to 08:42:00 UT, is shown in panel (a), for which purpose a box of 20 × 20 km was selected in the payload position (Fig. 5), and the mean intensity in the box has been plotted versus time. The electron count in situ data are shown in Fig. 8b, just below the relative auroral intensity. The correlation of the two curves (panels a and b) indicates the accuracy of the rocket position calculated. The increase in both auroral intensity and the electron count corresponds to the auroral arc crossed by the rocket at about 08:40:30 to 08:41:20 UT, indicated by the vertical lines. The rocket had a northward velocity 1 km/s and it crossed the arc at an the angle of about 45°, so the width of the arc-associated precipitation region can be estimated at about 40 km. Two precipitation peaks, indicated by letters (a) and (b), correspond well to respective auroral patches.

The following two panels, (c) and (d), show the electric field measured by the East payload, which indicates that the electric field increased in the auroral patches up to of the order of 20 mV/m in magnitude. The 200-km spatial periodicity in the electric field was concluded from the optical ground-based observations, electric field in situ measurements, and ground-based magnetic observations. The lower panels (e–i), in Fig. 8 show the magnetic field mea-

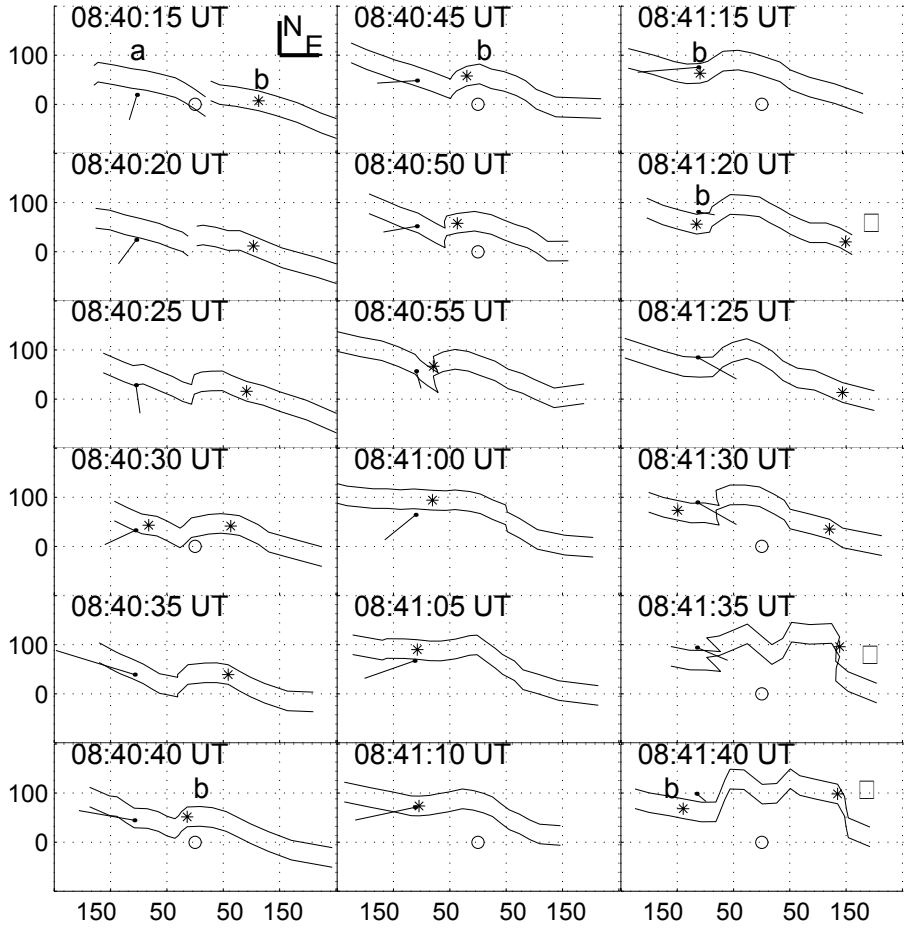

Fig. 6. On a geomagnetic grid (north is up and east is on the right), in kilometers, around Fort Yukon station (little circle at [0, 0] in Alaska/US the rocket position and a plasma convection flow (dot plus vector)). Using the method from Sect. 4 the auroral structure is sketched on the grid for 18 times out of a time interval from 08:40:15 to 08:41:40 UT on 11 February. The asterisks mark luminous regions inside the auroral arc structure. They are marked as **(a)**, **(b)** and **(c)**.

sured on the ground in PF and FY. In both observatories, the Y-component of the magnetic field shows 70-s pulsations, which corresponds well to the periodical variations in the northward plasma flow (eastward electric field) associated with moving auroral patches (Fig. 7b). Thus, the auroral patches and corresponding plasma flow form a 200-km periodic spatial structure that propagated westward at the velocity of the order of 3 km/s, which is indicated by the 70-s temporal pulsations observed on the ground.

To summarise this section, we will list the main features of the observed auroras:

1. The arc of about 40 km in width was stretched along the south-east direction at 20° to geomagnetic east. Inside the arc, ionospheric plasma velocity along the arc was 300 m/s westward, and convection reversal occurred at the northern edge of the arc.

2. Auroral patches and associated electric fields formed a 200 km periodical structure along the arc, which propagated westward at a velocity of 3 km/s. These bright patches coincide with equatorward plasma flow across the arc of the order of 200 m/s in magnitude, whereas at the intervals between the patches the plasma flow tends to be poleward. In the patches, the electric field reaches maximal magnitudes enhanced up to 20 mV/m.

5 Discussion

In this section we compare the characteristics of the observed auroral patches with the results obtained in earlier studies. It is important to mention that the earlier studies were mostly made in the morning side, where the auroral patches are commonly observed, whereas our observations were made in the evening side around 21:00 MLT, where such auroras are not typical and occur after a substorm (Royrvik and Davis, 1977). The main issues to be discussed are the precipitation mechanism, electric field pattern, and motion of the auroral patches.

Two basic mechanisms of auroral precipitation are known: (e.g. Swift, 1981) (1) acceleration by the field-aligned elec-

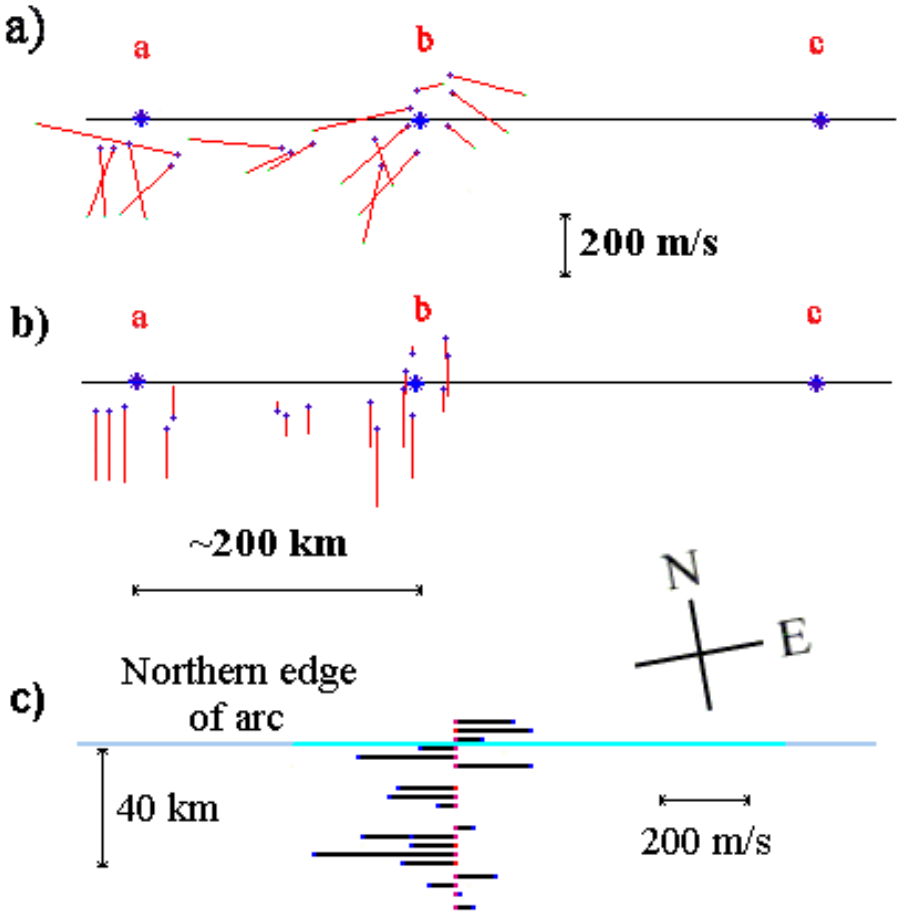

Fig. 7. Plasma drift velocity calculated from in situ electric field measurements, here presented as plasma flow (Fig. 6 in **(a)**, split up to components **(b)** plasma flows across the arc (Vx) and **(c)** plasma flows along the arc (Vy). The plasma drift velocity components are presenting arc-associated coordinate system (horizontal line; about 20 degrees offset from the geomagnetic coordinate system). The auroral patches marked in Figs. 5 and 6 are marked as (a), (b) and (c).

tric field associated with a field-aligned current (FAC) and (2) scattering of trapped particles into a loss-cone due to wave-particle interaction. The first precipitation mechanism should be associated with the field-aligned current flowing up from the luminosity area, and the corresponding convection vortex surrounding the patch (e.g. Kamide, 1981). However, our observations (Fig. 7b) indicate that the location of an upward FAC (associated with a clockwise vortex in Fig. 7a) is just westward of the patches, whereas the bright patches are associated with a maximum in the electric field magnitude (Figs. 8b and c) that suggest the absence of the field-aligned current. Thus, one can conclude that the observed auroral patches were caused by second mechanism, which agrees with the earlier results obtained mainly from observations of morning auroral patches. The patches were found to be associated with VLF emissions (e.g. Tagirov et al., 1999, and references herein). It has been concluded that the auroral patches are the result of pitch angle scattering of energetic electrons by magnetic whistler mode waves (Davidson, 1979; Tagirov et al., 1986). Our result suggests that the observed patches differ from the bright features in auroral arc elements studied earlier by Lanchester et al. (1996), who found that the regions of maximal luminosity and strong electric field are associated with FAC.

The second issue to be discussed is the electric field and convection pattern associated with the patches (Figs. 7b and 8b–d). Precipitation of the scattered energetic electrons results in the ionospheric conductivity increase and the corresponding polarization electric field (Maltsev et al., 1974; Mallinckrodt and Carlson, 1978; Kozlovsky and Lyatsky, 1997). Earlier ground investigations have shown that the patch-associated electric fields are induced in an ionisation tail in the ionosphere behind a moving auroral patch, in conjunction with the convection electric field (Oguti and Hayashi, 1984, 1985). A signature of this induced (polarization) electric field was observed in the course of the rocket-born measurement by Saito et al. (1992), who reported on the upward propagating kinetic Alfvén wave which was produced by the auroral precipitating electrons and the resultant ionisation of the neutral atmosphere. However, the polarization effect should result in an electric field magnitude diminished in the patches of enhanced ionospheric conduc-

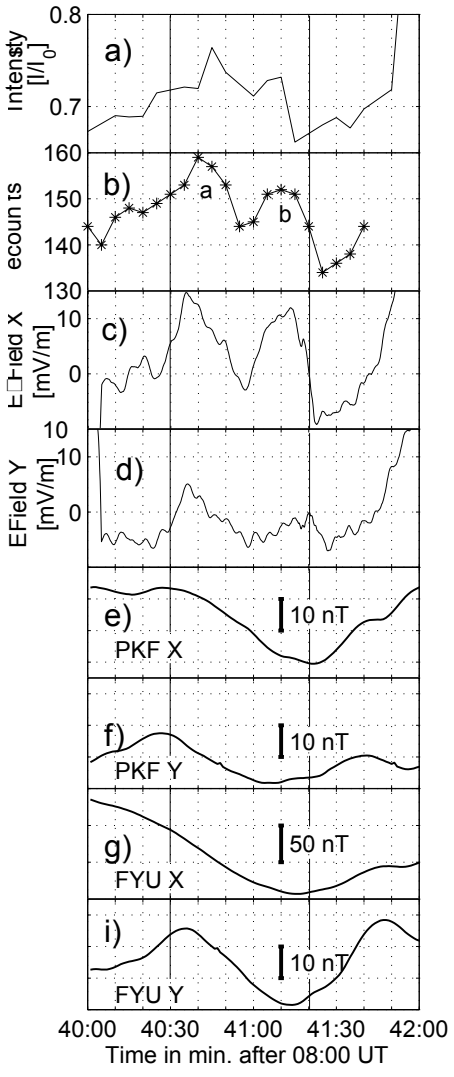

Fig. 8. AT2 in situ electron counts and relative intensity of the luminosity seen from ground as well as ground-based magnetic X- and Y-components at Fort Yukon and Poker Flat Alaska/US. All panels monitor the time from 08:40:00 to 08:42:00 UT on 11 February 1997. These times are equivalent to some of the times for the all-sky video frames seen in Fig. 4. The panels show (from top to bottom): the relative light intensity of the region of the rocket position seen from Fort Yukon, the rocket in situ electron counts, the rocket electric field Y- and X-components, ground magnetic X- and Y-component for Poker Flat and Fort Yukon.

tivity. On contrary, we observed clear increases in both the equatorward convection (Fig. 7b) and the electric field magnitude (Fig. 8) associated with the patch electron precipitations. Thus, one should suppose a magnetospheric source for the patch-associated electric field that will be discussed below.

We observed a westward motion of the auroral patches at the velocity of the order of 3 km/s, whereas the ionospheric plasma flow in the same direction did not exceed 300 m/s. This differs from the typical observed motion of the auroral patches, which, in many cases, was found to be governed by the magnetosphere-ionosphere convection ($\boldsymbol{E} \times \boldsymbol{B}$ drift) (e.g. Scourfield et al., 1983; Nakamura and Oguti, 1987). A difference in the velocities might be explained by assuming the inverted-V potential structure associated with the auroral arc along which the patches propagate. An other possible explanation is connected with a magnetospheric wave propagating westward. The wave model seems preferable, because it may explain both the fast westward propagation and the increased patch-associated electric field.

A suitable wave was studied theoretically by Maltsev and Lyatsky (1984a,b), where a dispersion equation was obtained for the surface waves at the sharp inner boundary of the plasma sheet, and the wave was suggested for the explanation of the east-westward motions of absorption bays. Further development was made in Safargaleev and Maltsev (1986), where the model has been expanded for the case of a diffuse boundary of the plasma sheet. To summarize the main results of the mentioned papers, in the magnetospheric regions, where a gradient of plasma pressure exists, the waves can propagate in the east-west direction (along the lines of constant plasma pressure). At the ionosphere level, these waves have a velocity of the order of several km/s and a wavelength of 100 km or larger, which is close to the characteristics reported here (3 km/s and 200 km, respectively). The wave propagation is associated with the plasma velocity oscillating in the north-south direction, which agrees well with our observations (Fig. 7b). And finally, the waves have an oscillating compressional component, which can change the anisotropy of trapped particles (in a compressing flux tube, the transverse temperature increases more than the parallel one). In its turn, the cyclotron instability growth rate depends on the anisotropy, so the compression may lead to the generation of a VLF wave. The generated VLF waves scatter hot electrons into the loss-cone that results in the precipitation (Hayashi et al., 1968; Coroniti and Kennel et al., 1970).

Magnetic field pulsations registered on the ground give additional evidence in favour of the wave. The period of the pulsations is consistent with the moving patches observed poleward of FY; however, the magnitude of the pulsation in FY was of the same range (about 10 nT) as in PF, located 200 km southward. This feature can be associated with a north-south oriented wave front rather than a magnetic effect of 100 km size patches.

Thus, we propose that the observed evening auroral patches may be due to the magnetospheric wave propagating in the boundary of the plasma sheet. On the other hand, the plasma sheet boundary is a favourable region for auroral arcs (e.g. Kozlovsky and Lyatsky, 1994, 1999), that is consistent with the observations in the evening sector development adaptation from arc segments into both discrete arcs and patches (Royrvik and Davis, 1977). Near the Earth ($L \leq 7\,R_E$), the sunward convection flow of hot particles splits, due to the gradient drift, so the hot ions drift westward to form the evening plasma sheet, whereas the energetic electrons drift to the east, where their precipitations produce morning auroral patches. Hence, the differences between the morning and evening patches follow from the dawn-dusk

asymmetry in the magnetospheric plasma.

6 Conclusion

We have investigated evening (around 21:00 MLT) auroral forms observed during the recovery of a substorm that occurred in the region of observations 23 min earlier. The observed auroral forms are discrete multiple auroral arcs stretched to the east and southeast from the breakup region, that are typical structures developing within the bulge expanding poleward during a substorm. At the substorm recovery, the arcs were decaying by developing into auroral patches and arc segments in a diffuse background, and bright auroral patches propagated westward along the arcs. We present a detailed investigation of the electric field and fine auroral structures associated with the arc, which was crossed by the sounding rocket in the course of AT2 experiment.

1. The arc of about 40 km in width was stretched along the south-east direction at 20° to geomagnetic east. Inside the arc, ionospheric plasma velocity along the arc was 300 m/s westward and convection reversal occurred at the northern edge of the arc.

2. Auroral patches and associated electric fields formed a 200 km periodical structure, which propagated along the arc westward at a velocity of 3 km/s, though they were moving much faster than the convection flow! This luminosity wave is a feature of the disturbed arc.

3. These bright patches were co-located with equatorward plasma flow across the arc of the order of 200 m/s in magnitude, whereas at the intervals between the patches the plasma flow tended to be poleward.

4. In the patches, the electric field reaches maximal magnitudes enhanced up to 20 mV/m, and the maxima were co-located with the peaks in electron precipitations, indicated by the electron counter on board the rocket.

5. Pulsations of a 70-s period were observed on the ground in the eastern component of the magnetic field, that is consistent with the velocity, spatial size, and convection pattern of the moving auroral patches.

The electric field measurements do not indicate that any field-aligned currents associated with the precipitations created the patches. The enhanced patch-associated electric field cannot be explained by the polarization effect, which, together with the fast westward propagation, suggests essential differences of the evening auroral patches from those occurring in the morning ionosphere. We propose the wave that propagates along the plasma sheet boundary to be a promising mechanism for the evening auroral patches.

Acknowledgement. We thank J. Kangas (Sodankylä Geophysical Observatory) for useful discussions. We acknowledge the Coordinated Data Analysis Web (CDAWeb) and the data provider, G. Parks (U. Washington) for the Polar Ultraviolet Imager data. This study was funded by the Vilho, Yrjä and Kalle Väisälä Foundation of the Finnish Academy of Science and Letters.

Without the wonderful teamwork of the Auroral Turbulence 2 rocket community, under the chair of R. Torbert (University of New Hampshire/USA) this work would have never been possible.

Topical Editor G. Chanteur thanks V. Safargaleev and another referee for their help in evaluating this paper.

References

Aikio, A. T., Opgenoorth, H. J., Persson, M. A. L., and Kaila, K. U.: Ground-based measurements of an arc-associated electric field, J. Atmos. Terr. Phys., 55, 797–808, 1993.

Akasofu, S.I.: The development of auroral substorm, Planet. Space Sci., 12, 273–283, 1964.

Coroniti, F. V. and Kennel, C. F.: Electron Precipitation Pulsations, J. Geophys. Res., 75, 7, 1279–1289, 1970.

Danielides, M. A., Ranta, A., Ivchenko, N., Jussila, J., Marklund, G., and Priemdahl, F.: Measurement of Auroral Characteristics by Auroral Turbulence II Sounding Rocket, Geophysica, 35, 1–2, 33–44, 1999.

Davidson, G. T.: Self/modulated VLF wave–electron interactions in the magnetosphere – A cause of auroral pulsations, J. Geophys. Res., 84, 6517–6523, 1979.

Davis, T. N.: Observed characteristics of auroral forms, Space Sci. Rev., 22, 77–223, 1978.

Elphinstone, R. D., Murphree, J. S., and Cogger, L. L.: What is a global auroral substorm?, Rev. Geophys, 34, 169–232, 1996.

Ivchenko, N., Marklund, G., Lynch, K., Pietrowski, D., Torbert, R., Primdahl, F., and Ranta, A.: Quasiperiodic oscillations observed at the edge of an auroral arc by Auroral Turbulence 2, GRL, 26, 22, 3365–3368, 1999.

Johnstone, A. D.: The mechanism of pulsating aurora, Ann. Geophysicae, 1, 4-5, 397–410, 1983.

Hayashi, K., Kokubun, S., and Oguti, T.: Polar chorus emission and worldwide geomagnetic variation, Rep. Ionos. Space Res. Japan, 22, 149–161, 1968.

Kamide Y.: Estimation of Ionospheric Electric Fields, Ionospheric Currents, and Field-Aligned Currents from Ground Magnetic Records, J. Geophys. Res., 86, A2, 801–813, 1981.

Kozlovsky, A. and Lyatsky, W.: Instability of the magnetosphere–ionosphere convection and formation of auroral arcs, Ann. Geophysicae , 12, 636–641, 1994.

Kozlovsky, A. and Lyatsky, W. B.: Alfvén wave generation by disturbance of ionospheric conductivity in the field–aligned current region, J. Geophys. Res., 102, A8, 17 297–17 304, 1997.

Kozlovsky, A. and Lyatsky, W.: Finite Larmor radius convection instability in the near–Earth plasma sheet, J. Geophys. Res., 104, A4, 2243–2449, 1999.

Lanchester, B. S., Kaila, K., and McCrea, I. W.: Relations between large horizontal electric fields and auroral arc elements, J. Geophys. Res., 101, A3, 5075–5084, 1996.

Lui, A. T. Y.: A multiscale model for substorms, Space Sci. Rev., 95, 325–345, 2001.

Lynch, K. A., Pietrowski, D., and Torbert, R.: Multiple-point measurements in a nightside auroral arc: Auroral Turbulence II particel observations, GRL, 26, 22, 3361–3364, 1999.

Mallinckrodt, A. J. and Carlson, C. W.: Relations between transverse electric fields and field-aligned currents, J. Geophys. Res., 83, 1426–1432, 1978.

Maltsev, Yu. P.; Leontynev, S. V., and Lyatskiy, V. B.: Pi2 pulsations as a result of evolution of an Alfvéen impulse orginating in the ionosphere during a brightening of aurora, Planet Space Sci., 22, 1519–1533, 1974.

Maltsev, Yu. P. and Lyatsky, W. B.: Surface waves on the plasma sheet boundary, Planet. Space Sci., 32, 12, 1547–1549, 1984a.

Maltsev, Yu. P. and Lyatsky, W. B.: Surface waves on the boundary of the plasma layer and Pi2 pulsations, Geomagnetism and Aeronomy, Engl. Transl.,24, 6, 800–803, 1984b.

Marklund, G.: Auroral arc classification scheme based on the observed arc-associated electric field pattern, Planet. Space Sci., 32, 2, 193–211, 1984.

Nakamura, R. and Oguti, T.: Drifts of auroral structures and magnetospheric electric fields, J. Geophys. Res., 92, 11 241–11 247, 1987.

Nakamura, R., Oguti, T., Yamamoto, T., and Kokubun, S.: Equatorward and poleward expansion of the auroras during substorms, J. Geophys. Res., 98, A4, 5743–5759, 1993.

Oguti, T. and Hayashi, K.: Multiple correlation between auroral and magnetic pulasations 2. Determination of electric currents and electric fields around a pulsating auroral patch, J. Geophys. Res., 89, 7467–7481, 1984.

Oguti, T. and Hayashi, K.: Polarization and wave forma of magnetic pulsations below pulsating auroras, Magnetic effects of electric currents inducted in an ionization tail of a moving auroral patch, J. Geomagn. Geoelectr., 37, 65–91, 1985.

Pietrowski, D., Lynch, K. A., Torbert, R. B., Marklund, G., Ivchenko, N., Ranta, A., Danielides, M., and Kelley, M. C.: Multipoint measurements of large DC electric fields and shears in the auroral zone, GRL, 26, 22, 3369–3372, 1999.

Rostoker, G., Akasofu, S.-I., Foster, J., Greenwald, R. A., Lui, A. T. Y., Kamide, Y., Kawasaki, K., McPherron, R. L., and Russell, C. T.: Magnetospheric substorms – Definition and signatures, J. Geophys. Res., 85, 1663–1668, 1980.

Rostoker, G.: The evolving concept of a magnetospheric substorm, J. Atmospheric and Solar-Terrestrial Physics, 61, 85–100, 1999.

Royrvik, O. and Davis, T. N.: Pulsating aurora – local and global morphology, J. Geophys. Res., 82, 4720–4740, 1977.

Safargaleev, V. V. and Maltsev, Iu. P.: Internal gravity waves in the plasma sheet, Geomagnetism and Aeronomy, Engl. Transl., 26, 220–223, 1986.

Saito, Y., Machida, S., Hirahara, M., Mukai, T., and Miyaoka, H.: Rocket observation of electron fluxes over a pulsating aurora, Planet. Space Sci., 40, 1043–1054, 1992.

Scourfield, M. W. J., Keys, J. G., Nielsen, E., Goertz, C. K., and Collin, H.: Evidence for the $\boldsymbol{E} \times \boldsymbol{B}$ drift of pulsating auroras, J. Geophys. Res., 88, 7983–7988, 1983.

Swift, D. W.: Mechanisms for auroral precipitation – A review, Rev. Geophys. and Space Phys., 19, 185–211, 1981.

Tagirov, V. R., Trakhtengerts, V. Iu., and Chernous, S. A.: The origin of pulsating auroral spots, Geomagnetism and Aeronomy, Engl. Transl.,26, 600–604, 1986.

Tagirov, V. R., Ismagilov, V. S., Titova, E. E., Arinin, V. A., Perlikov, A. M., Manninen, J., Turunen, T., and Kaila, K.: Auroral pulsations and accompanying VLF emissions, Ann. Geophysisicae, 17, 66–78, 1999.